ROBUST SHAPE PRIOR MODELING BASED ON GAUSSIAN-BERNOULLI RESTRICTED BOLTZMANN MACHINE

Han Zhang[1]*, Shaoting Zhang*[2]*, Kang Li*[3]*, Dimitris N. Metaxas*[1]

[1]Department of Computer Science, Rutgers University, Piscataway, NJ, USA
[2]Department of Computer Science, University of North Carolina at Charlotte, Charlotte, NC, USA
[3]Department of Industrial and Systems Engineering, Rutgers University, Piscataway, NJ, USA

ABSTRACT

Shape information is essential in medical image analysis as the anatomical structures usually have strong shape characteristics. Shape priors can resolve ambiguities when the low level appearance is weak or misleading due to imaging artifacts and diseases. In this paper, we propose a shape prior model based on the Gaussian-Bernoulli Restricted Boltzmann Machine (GB-RBM). This powerful generative model is effective in capturing complex shape variations and handling nonlinear shape transformations. The model also shows great robustness, which is able to handle both outliers and Gaussian noise with large variance. We validate our model on synthetic data and a real clinical problem, i.e., lung segmentation in chest X-ray. Experiments show that our shape modeling method is qualitatively and quantitatively better than other widely-used shape prior methods.

Index Terms— Shape prior, shape modeling, Gaussian-Bernoulli Restricted Boltzmann Machine, representation learning, segmentation

1. INTRODUCTION

Organ shape plays a crucial role in many clinical practices. Although appearance cues in medical images are the main evidence to derive shape models during segmentation, they may lead to fussy or misleading boundaries because of diseases and imaging artifacts. In this scenario, the high-level shape priors are effective in resolving the ambiguities and inferring the accurate shape boundaries from image appearances. There have been a large variety of approaches for shape prior modeling. The most commonly used shape model is Active Shape Model (ASM) [2], in which the shape variations are captured by principal component analysis (PCA). Various methods have been proposed to improve the shape prior module of ASM in the context of medical image analysis. They fall into three major categories: handling complex shape variations [1, 13], keeping local shape information [3, 11, 10] and resolving non-Gaussian errors [9]. However, most of them just focus on one or two aspects, and it is difficult to manage all of them simultaneously. Recently, Sparse Shape Composition (SSC) [14] has been proposed to tackle these three problems in an unified framework. It shows promising results in real clinical problems. However, SSC models shape prior as a linear combination of existing shapes. It is less effective in handling nonlinear transformations like partial stretching and bending.

On the other hand, Restricted Boltzmann Machine (RBM) and its extensions such as Deep Boltzmann Machine (DBM) have been successfully used to model binary shape images [4]. This model can preserve the local and global structure of the shape, and is able to generate samples which is different from images in the training set. However, we could hardly use this model directly in the medical image analysis due to two reasons: (1) Since the model can only capture the probability of each pixel being assigned to the shape region, it is not able to model the shape contour directly. This is not tractable when the image size is large, which is more widespread in medical image analysis. (2) Due to the complex model structure, especially in the small medical training dataset, it tends to have the overfitting problem, which makes the model sensitive to noises.

In this paper, we build a robust shape prior model based on the Gaussian-Bernoulli Restricted Boltzmann Machine (GB-RBM) for medical image segmentation. Different from RBM-based method, our method directly models shapes represented by contours or surfaces. The proposed model has the following merits. First, we impose sparsity constraints on the hidden units and force the model to learn a sparse-overcomplete representation of the shape. Therefore, in contrast to most PCA-based methods focusing on Gaussian errors, it is possible to simultaneously handle both outliers (gross errors) and Gaussian noise with large variance. Second, the nonlinear structure in our model makes it effective in capturing complex shape variations. Particularly, it is more robust to local shape transformations than SSC. Third, we propose an efficient shape refinement algorithm, which makes it possible to integrate our model with deformable models to yield an efficient segmentation framework. We apply this shape prior modeling method to both synthetic

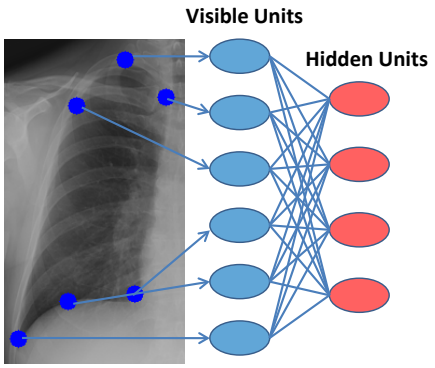

Fig. 1. Shape prior model based on GB-RBM.

data and real data, in particular, lung segmentation in chest X-ray. Our model shows better performance compared to the state-of-the-art methods.

2. SHAPE PRIOR MODELING VIA GB-RBM

The Restricted Boltzmann Machine (RBM) [12] is a powerful generative model. It has shown impressive performance in modeling binary shape images. However, biomedical images usually have a large number of pixels, making it impractical to model the probability of each pixel being assigned to the shape region. In this study, we propose to directly model the contour points of the organ shapes using a variant of RBM, i.e., the Gaussian Bernoulli Restricted Boltzmann Machine (GB-RBM) [7].

Model formulation: In our framework, we concatenate the coordinates of all contour points into a vector, denoted as $\mathbf{v} = [(x_{1,1}, x_{1,2}..., x_{1,k}), (x_{2,1}, x_{2,2}, ...x_{2,k}), ...(x_{n,1}, x_{n,2}, ...x_{n,k})]$, where n is the number of vertices in the shape and k is the dimension. Each shape vector $\mathbf{v}$ is pre-aligned using generalized Procrustes analysis [5] for transformation invariance. Then, the structure of the shape vector $\mathbf{v}$ can be represented by GB-RBM. As shown in Fig.1, our shape modeling is an undirected graphical model in which the visible shape units and hidden shape units form two layers of vertices in the graph. The hidden shape layer is a meaningful representation of the visible shape vector, which captures the underlying global and local structure of the shape. The corresponding energy function of our shape model is defined as:

$$\tilde{E}(\mathbf{v}, \mathbf{h}; \theta) = \frac{1}{2}\sum_i \frac{(v_i - b_i)^2}{{\sigma_i}^2} - \sum_{i,j} w_{ij} v_i h_j - \sum_j c_j h_j \qquad (1)$$

where $v_i \in R$ are the visible shape vector elements, $h_j \in \{0,1\}$ are the hidden shape units and w_{ij} are the connection strength between v_i and h_j. b_i and c_j are the bias weights for the visible shape units and hidden shape units. σ_i denotes the standard deviation of visible shape units. Under this definition, the distribution over visible shape units is given by marginalizing over hidden shape variables:

$$\tilde{p}(\mathbf{v}; \theta) = \frac{1}{\tilde{Z}} \sum_{\mathbf{h}} e^{-\tilde{E}(\mathbf{v}, \mathbf{h}; \theta)} \qquad (2)$$

where $\tilde{Z} = \sum_{\mathbf{h},\mathbf{v}} e^{-\tilde{E}(\mathbf{v}, \mathbf{h}; \theta)}$ is the normalizing constant.

Learning parameters: The model parameters are learned by minimizing the negative log-likelihood over the observed shapes. In addition, we impose sparsity constraints on the hidden units to avoid overfitting, since the training sets in medical image analysis are relatively small and well-structured. The sparsity in the hidden layer improves the robustness significantly. Therefore, our model can handle gross errors or outliers:

$$\arg\min_{\theta} \{ \sum_{k=1}^{m} -\log \tilde{p}(\mathbf{v_k}; \theta) + \beta KL(\rho || \hat{\rho}_k) \} \qquad (3)$$

where ρ is the sparsity parameter, $\hat{\rho}_k$ is the average activation of hidden units in training sample k and $KL(\rho||\hat{\rho}_k) = \rho \log \frac{\rho}{\hat{\rho}_k} + (1-\rho) \log \frac{1-\rho}{1-\hat{\rho}_k}$ denotes the Kullback-Leibler (KL) divergence between ρ and $\hat{\rho}_k$. β is the weight of sparsity penalty term. Although exact maximum likelihood learning for this model is intractable due to the normalizing constant $\tilde{Z}$, its optimization can be accomplished efficiently by Contrastive Divergence(CD) algorithm [6].

Parameter inference: Since our model has connections only between visible and hidden units, the conditional distributions needed for inference are factorial and computationally efficient:

$$p(h_j = 1 | \mathbf{v}) = \sigma(\sum_i W_{ij} v_i + c_j) \qquad (4)$$

$$p(v_i | \mathbf{h}) = \mathcal{N}(b_i + {\sigma_i}^2 \sum_j W_{ij} h_j, {\sigma_i}^2) \qquad (5)$$

Algorithm 1 k-step shape refinement

Input:
The corrupted shape $\tilde{\mathbf{v}} = [\tilde{v}_1, \tilde{v}_2, ...\tilde{v}_m]$;
The model parameter $\theta = \{\mathbf{W}, \mathbf{b}, \mathbf{c}, \boldsymbol{\sigma}\}$;
Output:
The refined shape $\mathbf{v} = [v_1, v_2, ...v_m]$;

$\mathbf{v^{(0)}} \leftarrow \tilde{\mathbf{v}}$
for $t = 1$ to k **do**
  for $j = 1$ to n **do**
    compute $p(h_j | \mathbf{v^{(t-1)}})$ by Eq.4
    sample $h_j^{(t)} \sim p(h_j | \mathbf{v^{(t-1)}})$
  end for
  for $i = 1$ to m **do**
    compute $p(v_i | \mathbf{h^{(t)}})$ by Eq.5
    sample $v_i^{(t)} \sim p(v_i | \mathbf{h^{(t)}})$
  end for
end for
return $\mathbf{v^{(t)}}$;

where $\sigma(y) = 1/(1+exp(-y))$ is the sigmoid function and $\mathcal{N}$ denotes Gaussian distribution. Thus the model can be viewed as a mixture of diagonal Gaussians with the number of components being exponential in the number of hidden shape units.

Shape refinement: Given a corrupted shape $\tilde{\mathbf{v}}$, the model can refine the shape efficiently by updating the hidden units $\mathbf{h}$ and the visible units $\mathbf{v}$ iteratively according to Eq. 4 and Eq. 5. The procedure is detailed in Algorithm 1. With this update scheme, our model can be used to refine the intermediate segmentation results, and hence improve the robustness of the segmentation algorithms.

3. EXPERIMENTS

3.1. Datasets and implementation details

Our dataset contains 186 chest X-ray images with the resolution around 2500×2500, obtained from different patients. Segmenting lung from chest X-ray is a challenging task, because the variation of lung shapes is very large due to differences caused by age, gender and lung disease. Among all the X-ray images, 30 cases are randomly selected for testing purpose, and the remaining is used for training. Ground truths are obtained by manual delineation of clinical experts.

In our experiment, 106 boundary points are evenly chosen in each lung shape to build the model. Our model has 1000 hidden units with the sparsity parameter $\rho = 0.01$. The weight of sparsity penalty term β is set to be 3. The total training is performed for 1000 epochs, which takes less than two minutes running on a dual-core, 2.4Ghz PC with 8GB memory in MATLAB implementation.

3.2. Lung shape refinement with synthetic noise

To evaluate the robustness of our shape prior model, we apply it to refine the corrupted shapes by synthetic noise. Specifically, Gaussian noise and outliers (gross errors) are used. In the first test, we add a large Gaussian noise $\varepsilon \sim \mathcal{N}(0, 160^2)$ on each boundary point of the shape. The standard deviation of the noise is almost five times that of the shape data. In the second test, we select a small proportion of points (e.g. 5/106) and add large gross errors (e.g. 60 times of the standard deviation of the data). Then we test our model against three methods: Procrustes Analysis (PA), SMS (the Shape Model Search in ASM, based on Principal Component Analysis) and SSC. To evaluate the performance of the shape refinement algorithms, we use the Dice Similarity Coefficient (DSC) [8], which is defined as: $2 \times TP/(2 \times TP + FP + FN)$, where TP, FP and FN denote true positive, false positive and false negative, respectively.

Fig.2 shows the results of shape refinement for different kinds of noise. Fig.2(a) indicates that all methods have a certain degree of robustness in handling gaussian error with large variance, and our model is slightly better than the other three.

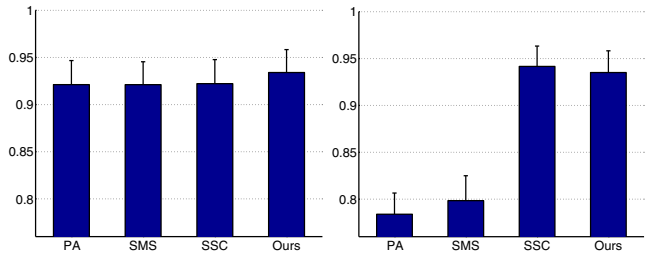

(a) Refinement for Gaussian error (b) Refinement for gross error

Fig. 2. Quantitative comparisons of shape refinement on synthetic data. The mean values ($\pm SD$) of DSC of different shape modeling methods are shown in the Figure. (a) the result of shape refinement for Gaussian error. (b) the result of shape refinement for gross error.

Fig.2(b) demonstrates that PA and SMS fail to handle gross errors in shape refinement. On the contrary, the result of our model is comparable to the SSC and they are both robust in handling such noise. Our model well handles both types of noise because of the following reasons. First, owing to the "S" shape of the sigmoid function in Eq.4, the state of hidden shape units is stable even when all the visible shape units are corrupted by Gaussian noise. Second, the sparsity constrains in the hidden shape layer improve the robustness even when a small proportion of visible units change greatly due to the gross error. Therefore, our model is able to recover a correct shape resulted from misleading appearance cues in images.

3.3. Lung segmentation from X-ray image

In this experiment, we segment the lung from chest X-ray images using deformable models and shape refinement. Our proposed shape prior modeling method is used to refine the intermediate results during the deformation procedure. Acting as a regularization step, it helps the deformable model avoid getting stuck in local minima of the image information. For comparisons, we also test the other shape prior modeling methods (e.g. SMS, SSC) to refine shapes after several iterations. To evaluate these methods on handling local shape transformations, we add partial bending on some of the testing data. Our proposed method improves the DSC of intermediate segmentation results by 3 percent, whereas the improvements of SSC and SMS are 1.5 and 1 percent, respectively. This experiment shows that both SMS and SSC are unsatisfactory in capturing the local shape information due to the linear structure in these models. On the contrary, our model can successfully keep the local shape constraints. The reason is that the nonlinear activation function of the hidden units allows the model to capture complex shape variations. In addition, the hidden shape layer forms a sparse-overcomplete representation of the shape, and some hidden shape units preserve the local shape details and help the model to generate a reasonable shape. Evaluated on all our testing data, the pro-

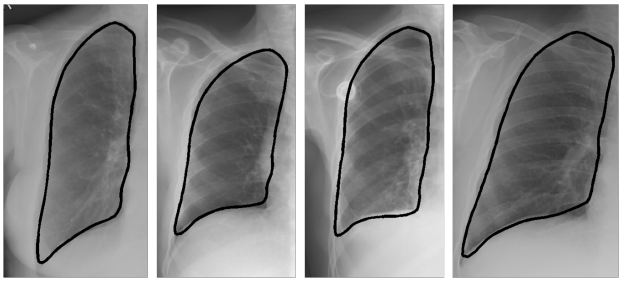

Fig. 3. Shape refinement on intermediate segmentation results using our method

posed method achieves the best performance compared to the other shape refinement approaches. Specifically, DSC of our method is 0.97, which is better than the same segmentation framework with SSC (DSC 0.956) and SMS (DSC 0.939). Fig.3 shows some shape refinement results using our method, which demonstrates that it works well on diverse shapes. Our shape refinement algorithm is also very efficient. It only takes 0.02s to refine the shape per iteration, while SSC takes 2.51s for the same task. Although Dictionary Learning method can be employed to improve the speed of SSC [15], it still needs to solve a convex optimization problem, which is not as efficient as our method. In our experiment, the proposed method not only improves the robustness of deformable model, but also enhances the efficiency of deformation by avoiding local minima of image information.

4. CONCLUSION AND FUTURE WORK

In this paper, we proposed a robust shape prior modeling method based on GB-RBM. It shows great robustness to both outliers (gross errors) and Gaussian noise. Benefited from the nonlinear shape embedding in our model, it is able to handle local shape transformations, e.g. partial bending and stretching. In addition, we proposed an efficient shape refinement algorithm and it can be combined with deformable models to segment region-of-interest efficiently. We validated our model on the synthetic and real data of chest X-ray. Experiments show that our shape modeling method are both qualitatively and quantitatively better than other widely-used shape prior methods. In the future, we plan to validate our method on large scale datasets and extend the method to 3D images. We are also interested in using the deep extensions of GB-RBM to build a hierarchical shape prior model.

This work is partially supported by grant NSF-MRI-1229628.

5. REFERENCES

[1] T. Cootes and C. Taylor. A mixture model for representing shape variation. *Image and Vision Computing*, 17(8):567 – 573, 1999.

[2] T. Cootes, C. Taylor, D. Cooper, and J. Graham. Active shape model - their training and application. *CVIU*, 61:38–59, 1995.

[3] C. Davatzikos, X. Tao, and D. Shen. Hierarchical active shape models, using the wavelet transform. *TMI*, 22(3):414–423, 2003.

[4] S. Eslami, N. Heess, and J. Winn. The shape boltzmann machine: A strong model of object shape. In *Computer Vision and Pattern Recognition (CVPR), 2012 IEEE Conference on*, pages 406–413, 2012.

[5] C. Goodall. Procrustes methods in the statistical analysis of shape. *JRSS*, 53:285–339, 1991.

[6] G. E. Hinton. Training products of experts by minimizing contrastive divergence. *Neural computation*, 14(8):1771–1800, 2002.

[7] G. E. Hinton and R. R. Salakhutdinov. Reducing the dimensionality of data with neural networks. *Science*, 313(5786):504–507, 2006.

[8] A. Popovic, M. de la Fuente, M. Engelhardt, and K. Radermacher. Statistical validation metric for accuracy assessment in medical image segmentation. *International Journal of Computer Assisted Radiology and Surgery*, 2(3-4):169–181, 2007.

[9] M. Rogers and J. Graham. Robust active shape model search. In *ECCV*, pages 517–530, 2002.

[10] D. Seghers, D. Loeckx, F. Maes, D. Vandermeulen, and P. Suetens. Minimal shape and intensity cost path segmentation. *TMI*, 26(8):1115–1129, 2007.

[11] K. Sjostrand, E. Rostrup, C. Ryberg, R. Larsen, C. Studholme, H. Baezner, J. Ferro, F. Fazekas, L. Pantoni, D. Inzitari, and G. Waldemar. Sparse decomposition and modeling of anatomical shape variation. *TMI*, 26(12):1625–1635, 2007.

[12] P. Smolensky. Parallel distributed processing: explorations in the microstructure of cognition, vol. 1. chapter Information processing in dynamical systems: foundations of harmony theory, pages 194–281. MIT Press, Cambridge, MA, USA, 1986.

[13] P. Yan, S. Xu, B. Turkbey, and J. Kruecker. Discrete deformable model guided by partial active shape model for trus image segmentation. *IEEE Trans. Biomed. Eng*, pages 1158–1166, 2010.

[14] S. Zhang, Y. Zhan, M. Dewan, J. Huang, D. N. Metaxas, and X. S. Zhou. Towards robust and effective shape modeling: Sparse shape composition. *MedIA*, 16(1):265 – 277, 2012.

[15] S. Zhang, Y. Zhan, and D. N. Metaxas. Deformable segmentation via sparse representation and dictionary learning. *MedIA*, 16(7):1385 – 1396, 2012.